Journal of Fluids and Structures (1990) **4**, 345–370

AERODYNAMIC SOURCES OF ACOUSTIC RESONANCE IN A DUCT WITH BAFFLES

K. HOURIGAN, M. C. WELSH AND M. C. THOMPSON
Commonwealth Scientific and Industrial Research Organisation, Division of Building, Construction and Engineering, Highett, Victoria, 3190, Australia

AND

A. N. STOKES
Commonwealth Scientific and Industrial Research Organisation, Division of Mathematics and Statistics, Clayton, Victoria, 3168, Australia

(Received 21 June 1989 and in revised form 12 January 1990)

Experimental and numerical investigations of the generation of resonant sound by flow in a duct containing two sets of baffles and the "feedback" of the sound on the vortex shedding process are reported. The experiments are conducted in a wind tunnel and the numerical simulations are used to predict the sources of resonant sound in the flow. The resonant sound field, which is principally longitudinal, is calculated by the finite element method and a discrete-vortex model is used to predict the observed separated flow. Analysis of the passage of a single point vortex past a baffle indicates that the amount of acoustic energy generated is a function of the phase of the acoustic cycle at which the vortex passes the baffle. A more elaborate model simulates the growth of vortex clouds through the clustering of elemental vortices shed from an upstream baffle, tracks the passage of these vortex clouds past a downstream baffle, predicts the generation of acoustic energy using Howe's theory of aerodynamic sound, and accounts for the feedback of sound on the vortex shedding. Comparison is made between the predicted time-dependent structures and the observed flow structures using smoke visualization. The vortex cloud model predicts the flow conditions under which net acoustic energy is generated by the flow and therefore when resonance can be sustained; the results are consistent with the occurrence of peaks in the observed resonant sound pressure levels.

1. INTRODUCTION

THE EXCITATION OF ACOUSTIC MODES IN THE combustion chamber of solid-propellant rocket motors can lead to uncontrolled burning and vibration problems (Hegde & Strahle 1985). Large flange-type structures inserted between segments of grains can result in strong shear layers which interact with similar structures downstream, resulting in a self-sustained oscillating system (Brown *et al.* 1981).

An experimental investigation of the acoustic oscillations sustained by a flow through a duct with two sets of baffles, representing an idealized solid-propellant combustion chamber, has been carried out by Nomoto & Culick (1982). It was found that pure acoustic tones corresponding to longitudinal resonant modes of a duct were generated for certain flow and geometrical conditions. When the acoustic tones were present, the frequency of the vortex shedding from the upstream baffles was synchronized with a natural acoustic frequency of the duct. However, acoustic feedback was dismissed as a means of inducing the observed vortex shedding.

0889–9746/90/040345 + 26 $03.00

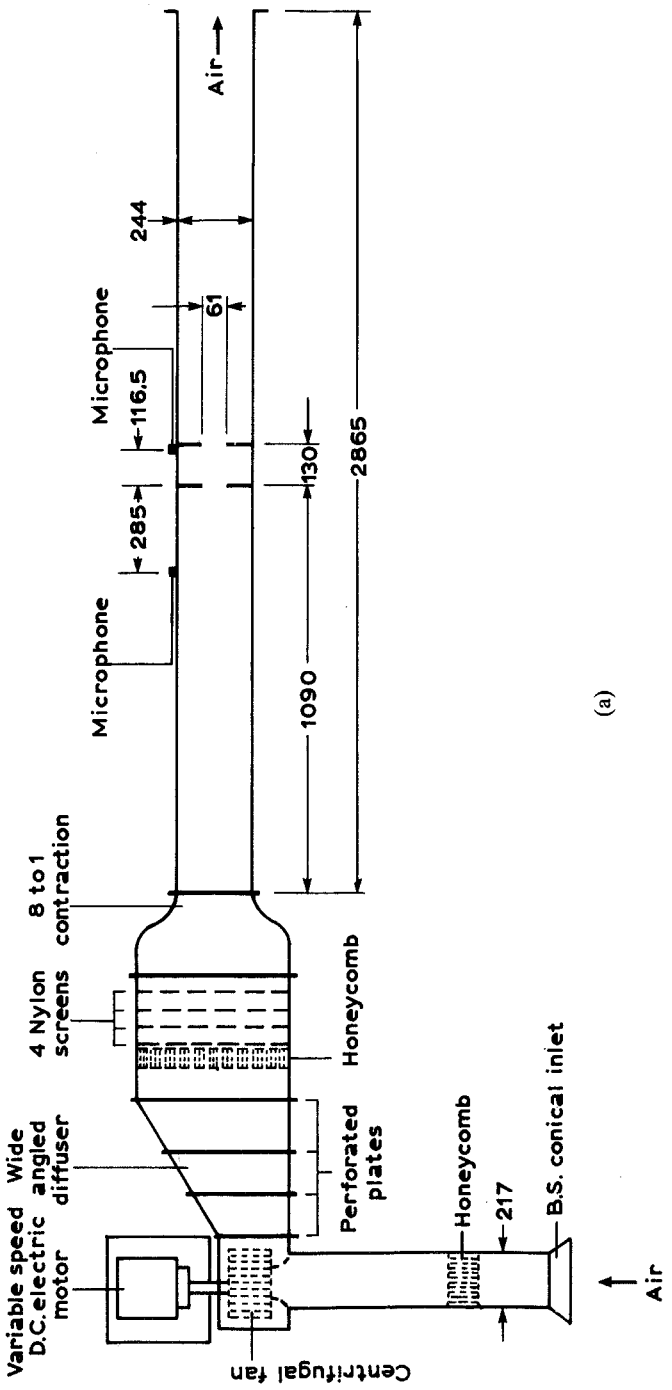
Air
244
61
Microphone
116.5
285
Microphone
130
2865
1090
8 to 1 contraction
4 Nylon screens
Honeycomb
Wide angled diffuser
Perforated plates
Honeycomb
217
B.S. conical inlet
Variable speed D.C. electric motor
Centrifugal fan
Air

(a)

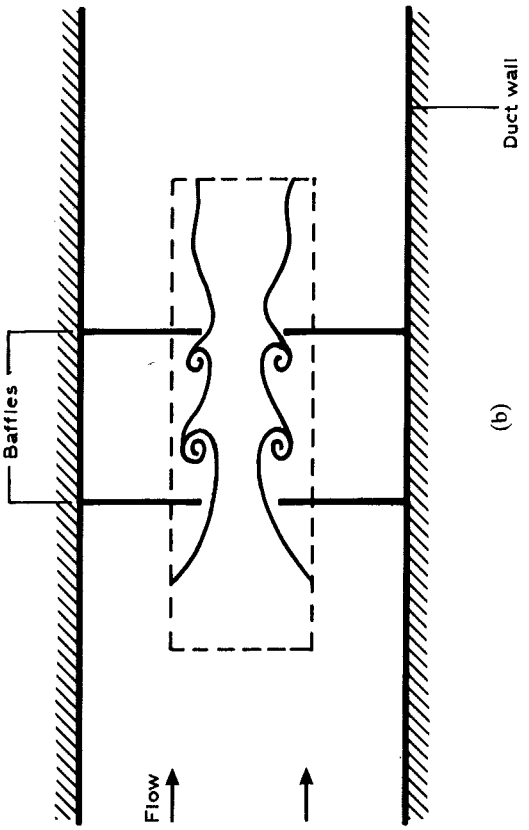

Figure 1. (a) Schematic of the test rig; (b) schematic of the working section showing region of flow visualisation (broken lines) corresponding to photographed region in Figure 6.

The aim of this paper is to describe the resonant acoustic sources in a duct containing baffles (in terms of the flow and the acoustic field near the baffles) using Howe's (1975) theory of aerodynamic sound. Figure 1 shows schematics of the test rig and working section. Furthermore, the paper aims to establish whether acoustic feedback is the mechanism which synchronizes the vortex shedding. The background to the present study is presented in Section 2. Section 3 describes the experimental apparatus and the procedures used for measuring the resonant acoustic sound and photographing the flow. Descriptions of the finite element method for predicting the acoustic field, two flow models and the aeroacoustic theory of Howe (1975) relevant to the problem are presented in Section 4. Sections 5 and 6 cover the results and discussion pertaining to both the experimental and the computational investigations. The predicted resonant acoustic field and the acoustic Strouhal numbers at which acoustic resonance is observed are presented. Only the case for the simplest acoustic mode which can be excited, corresponding to that with a wavelength approximately equal to the length of the working section, is described. To illustrate qualitatively the sound generation mechanism, a simplified flow model with a single vortex passing a baffle is presented. This model indicates how the flow near the downstream baffle can act as an acoustic source region, provided the vortices pass the baffle at the appropriate phase in the sound cycle. In the second model, the flow is represented as the sum of a steady potential flow, a flow with vortex clouds in free motion, and an oscillating flow representing the acoustic field. The vortex cloud model additionally accounts for the feedback of the resonant sound on the vortex shedding from the upstream baffle and predicts the acoustic Strouhal numbers at which peaks occur in the acoustic energy per cycle generated by the flow. Individual vortex structures are also tracked to show their role in sustaining the acoustic resonance at favourable acoustic Strouhal numbers. The predictions are compared with experimental results. Section 7 sets out the conclusions of the study.

The major result of the study is that a feedback loop can be established between a resonant sound field and the vortex shedding from a set of baffles in a duct. Although this loop can be established over a number of flow velocity ranges, the common factor leading to the maintaining of the loop is the phase of the acoustic cycle when each vortex arrives at the downstream baffles. It is only for particular ranges of flow velocities that the phasing between the vortex passing the downstream baffle and the resonant acoustic field is such that sufficient positive net acoustic energy is generated to sustain the acoustic resonance and the feedback loop.

2. BACKGROUND

Flow induced acoustic resonances in ducts can manifest in different modes depending on various factors, including duct modification and flow velocity. For simple rectangular ducts, the modes can be classified as either transverse or longitudinal, depending on the general direction of the wave motions. Single or multiple sources of sound are found for the transverse modes; the major source of sound may or may not be remote from the point of vortex shedding to which the sound feeds back and controls. Generally, longitudinal modes are excited by acoustic sources remote from the point of vortex shedding.

A brief review of some previous investigations involving different modes and source regions is presented in this section.

2.1. Excitation of Transverse Duct Acoustic Modes

Parker (1966) and Parker & Griffiths (1968) made detailed studies of acoustic resonances induced by vortex shedding from vertical cascades of plates located in horizontal flow ducts; the resonances were excited purely by the flow and did not require structural vibration for their excitation (Parker 1969). Parker (1967) also predicted the resonant frequencies by solving the wave equation for the space surrounding the plates. He showed that the frequencies depend on the dimensions of the plate as well as the dimensions of the duct. The simplest acoustic mode was defined to be the β-mode which describes the acoustic field both near the plate and in the far field, where it becomes an evanescent cross-mode of the duct. Later studies of acoustic resonance by Cumpsty & Whitehead (1971), Archibald (1975), Welsh & Gibson (1979) and others observed resonances when a single plate was installed in a duct.

2.1.1 *Acoustic source coincident with vortex shedding region*

Welsh *et al.* (1984) reported a more detailed study of the excitation of acoustic resonances in flow around plates with semicircular leading edges. They examined the fluid mechanics of the resonant process in a duct containing a plate with a semicircular leading edge. The process is described in terms of an interchange of energy between the flow and acoustic fields and has three basic components: (a) an acoustic source (the vortex street); (b) a feedback effect of the sound on the vortex shedding; and (c) a damping process whereby acoustic energy is transferred out of the duct system. This study showed that there was an acoustic source downstream of the trailing edge where vigorous vortex shedding occurred.

2.1.2. *Acoustic source remote from vortex shedding region*

Single square leading edge plates

Welsh & Gibson (1979) examined the interaction between resonant sound and vortex shedding from a flat plate with a square leading edge. They found that only those acoustic modes with acoustic velocity antinodes near the plate and the associated vortex street were excited by the vortex shedding. They also found that plates with square leading edges could shed large-scale vortices from either the leading edge or the trailing edge during resonance, and showed that the same acoustic mode could be excited at the same frequency over several ranges of flow velocity.

Stokes & Welsh (1986) modelled the acoustic resonance process for the case of plates with square leading edges. The mathematical model showed that in resonance, the vortices observed shedding from the leading edge during each acoustic cycle generated a net supply of acoustic energy as they passed the trailing edge, provided the passage was at a particular phase of the sound cycle. A variety of solutions was found to exist for the number of sound cycles that may pass while a vortex travels from the leading edge to the trailing edge so that it arrives there at the appropriate phase in the sound cycle. Correspondingly, there are several ranges of flow velocity at which this phase can be achieved to generate a net supply of acoustic energy. These predicted flow velocity ranges closely coincided with the velocity ranges for which acoustic resonance is observed in practice (Stokes & Welsh 1986). Since a vortex is shed each acoustic cycle during resonance, each velocity range corresponds to a different number of vortices observed at a particular instant between the leading and the trailing edges.

More recently, Welsh *et al* (1990) have observed that, similar to the case of square leading edge plates, vortices are shed from semicircular leading edges of plates, and that this vortex shedding can excite, and in turn be synchronised by, a transverse duct mode.

In all of these cases, a strong acoustic source was present downstream of the region where vortex shedding was synchronized by the resonant sound.

Multiple plates

If two plates with semicircular leading edges are placed in tandem in a duct, a resonant transverse acoustic mode of the duct can be excited, leading to feedback of the sound onto the separating shear layers at the trailing edge of the upstream plate (Stoneman *et al*. 1988). The amplitude of the sound can be substantial, resulting in the locking of the vortex shedding to the resonant sound frequency. The periodic reappearance of loud acoustic resonances as the plate spacing was increased is similar to that observed for single plates with blunt leading edges as the flow velocity was decreased. In both cases, resonance relied on the vortices shed upstream passing either a trailing edge or a second plate at an appropriate phase of the acoustic cycle.

2.2. Excitation of Longitudinal Duct Acoustic Modes

Nomoto & Culick (1982) published data showing vortex shedding exciting acoustic resonances in rectangular ducts containing two pairs of baffles; as distinct from transverse resonance modes investigated by Stokes & Welsh (1986) and Stoneman *et al*. (1988), the resonances were essentially the longitudinal organ pipe modes of the duct. As for the case described above of the plate with a square leading edge, Nomoto & Culick (1982) observed the same resonant acoustic mode being excited over several different ranges of flow velocity. Again, each range was uniquely characterized by the number of vortices observed between the baffles at a given instant. Harris *et al*. (1988) investigated the air flow through a double orifice in a pipeline; acoustic resonance in the pipe mode could be excited at particular flow velocities, and shear layer oscillations leading to the formation of large-scale vortex structures at the resonant frequency were observed.

Some flow geometries, such as jet-edge interactions, lead to self-sustaining oscillations by purely hydrodynamic perturbations (Rockwell 1983); the accompanying sound produced by the flow oscillations is not amplified by duct reflections. However, the frequencies of the oscillations and consequent sound are functions of the flow velocity, whereas in the present case, the vortex shedding and sound frequencies are predominantly a function of the duct geometry and involve loud resonant sound levels. This suggests that for the current investigation, the influence of sound on the development of flow structures is important and that the mechanism leading to the oscillation is fundamentally different to that proposed by Rockwell (1983) for a different flow. Nomoto & Culick (1982) cast doubt on the influence of resonant sound on the vortex shedding process for flow in a duct geometry similar to the present investigation, in which the flow is reexamined experimentally and theoretically. Chung & Sohn (1986) and Flandro (1986) investigated the coupling mechanism of acoustic and vortical wave oscillations in connection with rocket combustion chambers using linear stability theory. Their results, which are relevant only to the initial excitation of an acoustic resonance, clearly indicate that a feedback loop can be established between the sound field and the growth of instabilities in the shear layer. The present work,

following Stokes & Welsh (1986) and Stoneman *et al.* (1988), is concerned with the non-linear coupling of finite resonant acoustic waves and vortex shedding which is observed when a loud acoustic resonance has been excited.

2.3. Determination of the Acoustic Sources

In the studies of Welsh *et al.* (1984), Stokes & Welsh (1986) and Stoneman *et al.* (1988), and in the present study, the source of acoustic energy due to the vortex street is modelled using Howe's (1975, 1980) theory of aerodynamic sound. According to this theory, the acoustic power generated by a vortex as it passes through a sound field is proportional to the scalar triple product of the vorticity, the velocity of the vortex and the acoustic particle velocity. For low Mach number flows the acoustic and flow fields can be decoupled and solved for separately. Then, assuming a resonant sound field is present, the acoustic power generated by a vortex passing through it can be computed using Howe's theory. If, on integrating the power over time, there is a net source of acoustic energy then resonance is possible, provided damping is overcome. However, a net negative source of energy implies that a resonance is not sustainable.

It is the purpose of this paper to show that the acoustic sources in a flow around baffles in a duct can be examined in a manner analogous to the flows around plates, even though the excited resonant acoustic mode is longitudinal rather than transverse.

3. EXPERIMENTAL APPARATUS AND PROCEDURES

The experimental apparatus was a small blow down wind tunnel, shown schematically in Figure 1(a). A British Standard conical inlet 217 mm in diameter was connected to the fan inlet for monitoring the volume flow through the tunnel. A wide angle diffuser containing four perforated plates connected the fan to the settling chamber which consisted of a honeycomb and four fine nylon screens. From the settling chamber, air passed through an 8 to 1 contraction before entering the working section, which consisted of rigid ducting with internal dimensions of 244 mm square. The total length of the 244 mm square ducting was 2865 mm. Some portions of the modules were constructed from 12 mm thick aluminium and contained facilities for mounting microphones flush with the inside surface of the duct, while other parts of the ducting were constructed from 25 mm and 50 mm thick acrylic (methyl-methylacrylate) sheets with optical glass inserts for flow visualization (Figure 1b). A chamber 130 mm long in the flow direction was formed midway along the ducting by installing two pairs of baffles across the flow inside the ducting. The opening between the baffles was 61 mm, which was 25% of the full duct width.

The velocity profile approaching the baffles was uniform (within 1%) between the wall boundary layers, which were approximately 15 mm thick. The axial component of the turbulence intensity in the core of the flow was 0·3% with significant spectral content less than 100 Hz.

Acoustic resonances were identified by recording the signal from a fixed 12·7 mm diameter Brüel and Kjaer microphone mounted flush with the surface inside the chamber (Figure 1). This microphone was located near a duct corner in a plane 116·5 mm downstream of the upstream baffle. A second Brüel and Kjaer microphone was located near a duct corner and 285 mm upstream of the upstream baffle. The flow and acoustic variables were recorded for the maximum sound pressure level for each resonance as the mean flow velocity upstream of the baffles was increased from zero to

5 m/s. The resonance frequencies were obtained by performing a ninth order fast Fourier transform with ten averages on the microphone data.

The sound pressure levels at the acoustic resonance frequency were determined from narrow band analysis (bin width of 1·95 Hz) of the microphone signals. Since these signals were tonal and up to 40 dB above the background, the amplitude of the spectral peak approximated the sound pressure level at the required frequency. The amplitude of the spectral peak was calibrated using an input signal of known sound pressure level from a Brüel and Kjaer piston phone.

The phase relationship between the vortices and the acoustic field was determined by introducing smoke into the working section upstream of the baffles and photographing the flow at selected points in the acoustic cycle using a time delay unit connected to the microphone signal. The flash photographs shown in this paper were obtained by superimposing ten exposures taken for the same flow conditions, $0{\cdot}16 \pm 0{\cdot}03$ of an acoustic cycle before the minimum acoustic pressure was reached at the microphone upstream of the baffles [Figure 1(a)].

4. THEORY AND MATHEMATICAL MODELLING

In the following mathematical models, the ducts and baffle geometries are based on the test rig shown in Figure 1(a). As a result of the symmetry of the flow and the acoustic field about the mid-line of the duct, only one half of the duct flow is explicitly modelled.

4.1. Acoustic Field

The acoustic mode to be modelled is a standing wave corresponding to an organ pipe mode. In the flows of interest here, the Mach number is small and the acoustic pressure p satisfies the wave equation:

$$\frac{\partial^2 p}{\partial \tau^2} = c^2 \nabla^2 p \tag{1}$$

where c denotes the velocity of sound and τ is time.

The time-dependent amplitude function ϕ can be extracted from a standing wave solution $p = \phi e^{i2\pi f\tau}$, where f is the frequency. Then ϕ satisfies the Helmholtz equation:

$$\nabla^2 \phi + (2\pi f/c)^2 \phi = 0. \tag{2}$$

For the low frequency modes, which are symmetrical about the horizontal midplane, the following boundary condition applies on the rigid surfaces and also on the midplane:

$$\mathbf{k} \cdot \nabla \phi = 0, \tag{3}$$

where $\mathbf{k}$ is the unit vector normal to the surface. The boundary conditions at the ends of the working section of the duct are, in reality, more complex due to the presence of other surfaces in the wind tunnel. However, as Blevins (1985) has also found, the solutions in the inner region of the duct where the baffles are located are insensitive to whether Dirichlet or Neumann conditions are used for the end boundary pressures. In the present study, the Dirichlet condition at the ends, i.e. $p = 0$, is employed.

For the simplified single vortex model of the flow, the sound field, which has a long wavelength compared with the dimensions of the baffles, is approximated locally by the

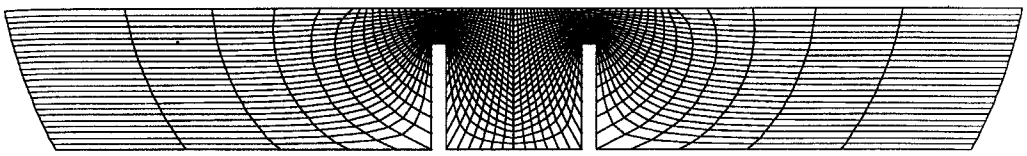

Figure 2. Part of the mesh used for finite element prediction of the acoustic field.

potential flow solution around a baffle determined using the conformal transformations described below in Section 4.2.1.

For use in the vortex cloud model, the boundary value problem is solved by the finite element method using rectangular elements and piecewise linear shape functions. The orthogonal mesh used, shown in Figure 2, is compressed near the tips of the baffles and is generated using a finite difference method solved by line successive over-relaxation. The method, due to Warsi (1982), is based on the idea that different coordinate systems in a given region should be related by the transformation laws of tensors. The lowest frequency acoustic mode is found by an iteration procedure in which the eigenvalue is estimated at each step by the Rayleigh quotient (e.g. Zienkiewicz 1978). Successive higher modes can then be found in a similar manner.

4.2. Flow Modelling

4.2.1. *Single vortex model*

This model is used to investigate the resonant acoustic power generated by a single point vortex passing an isolated baffle in duct. The model assumes a two-dimensional inviscid incompressible flow, irrotational everywhere except at the centre of the point vortex. For simplicity, the vortex of infinitesimal strength is assumed to follow a horizontal path with velocity determined by the horizontal components of the irrotational flow velocity and the induced velocity due to the image vortex. Since the working section is long compared with the flow features, its length is assumed infinite. The transformation which takes the complex potential w for a flow past a set of thin baffles into the variable z, which represents the points in the physical plane, is given by

$$z = -\frac{d}{\pi}\log\left(\frac{\cos a - v}{\cos a + v}\right), \tag{4}$$

where $v = (\tanh^2 w - \sin^2 a)^{\frac{1}{2}}$, a is the baffle height and d is the spacing between the duct walls.

4.2.2. *Vortex cloud model*

In this model, the flow is modelled by a two-dimensional inviscid incompressible flow, irrotational everywhere except at the centres of elemental vortices. Due to the symmetry of the flow and the resonant acoustic field about the longitudinal centreline of the duct, only the flow in the lower half duct is explicitly modelled. The shedding of vorticity is modelled by the creation of the elemental vortices, which are convected under the influence of other elemental vortices and the irrotational flow.

In the single vortex model, no attempt was made to simulate the process of vortex formation through instability in separating shear layers. However, in this section, the vortical flow around the baffles in the duct, which includes the instability of the separating shearlayer, is modelled by releasing elemental vortices from the surfaces of

the baffles and tracking their motions as they evolve into clouds. To satisfy the rigid duct wall condition, a similar mapping to that employed for the single vortex calculation described in Section 4.2.1 was used. This mapping $w = e^z$ transformed the duct into a half-plane (λ-plane) and the vortex-induced perturbations were forced to meet the duct-wall conditions by introducing mirror images. The no slip boundary condition was satisfied at the baffle surfaces through the surface vorticity method (Lewis 1981). Figure 3 shows the baffle geometry in the original z-plane and transformed λ-plane.

The surface vorticity method has been used previously by Lewis (1981) and Stoneman *et al.* (1988), amongst others, to represent the surface of a bluff body by a vortex sheet. In brief, it is required that the contour along the body surface is a streamline and that the tangential velocity on the inside of the vortex sheet is zero. Denoting the distance along the body surface by s, discretization of a vortex sheet into M segments, with the nth segment having length Δs_n and linear vorticity density $\gamma(s_n)$, produces a set of linear equations,

$$\sum_{n=1}^{M} \gamma(s_n)K(s_n, s_m)\Delta s_n - \tfrac{1}{2}\gamma(s_m) = -(v_x + v_{x,a})\left(\frac{\mathrm{d}x_m}{\mathrm{d}s}\right) - (v_y + v_{y,a})\left(\frac{\mathrm{d}y_m}{\mathrm{d}s}\right) - \sum_{n=1}^{N_v} \Gamma_n T(n, s_m), \qquad (m = 1, M), \tag{5}$$

where the last term in equation (5) gives the contribution to the velocity field at the surface due to N_v free vortices of circulation Γ in the flow. The coupling coefficient $K(s_n, s_m)$ has the value of the surface tangential velocity at s_m induced by a vortex of unit circulation at s_n. The coupling coefficient $T(n, s_n)$ has the value of the surface

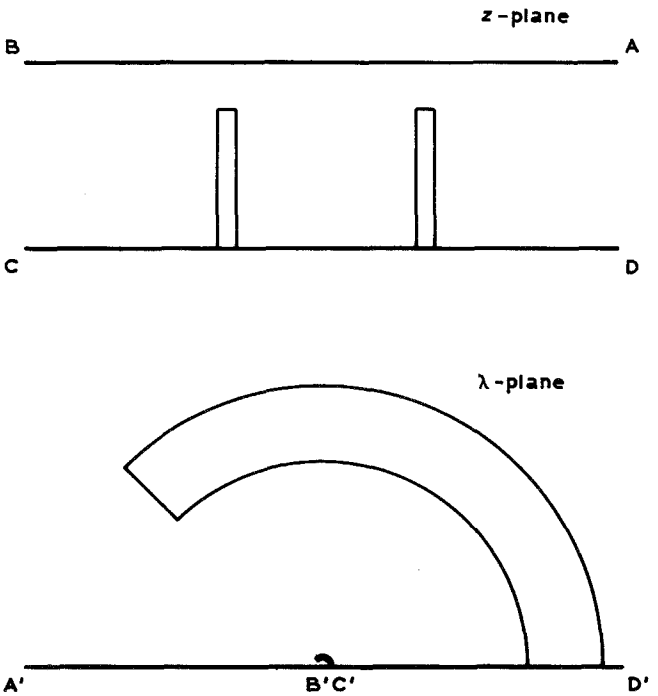

Figure 3. Transformation used in the vortex cloud model mapping the half duct to a half plane together with the baffle geometries in each plane.

tangential velocity at s_m due to a vortex of unit circulation at the position of the nth free vortex. The velocity of the irrotational flow has been separated into a steady component (v_x, v_y) and an unsteady component ($v_{x,a}$, $v_{y,a}$) contributed by the acoustic field; owing to the long wavelength of the acoustic field relative to the dimensions of the vortex structures, the flow due to the acoustic field is almost potential locally in the region of the baffles and is incorporated into the potential flow. The solution of (5) gives the surface vorticity density at the pivotal points on the surface of the body, which are taken to be the centre of each discrete element.

In the scheme used by Stoneman *et al.* (1988), elemental vortices were released into the flow from a very limited number of designated flow separation points. In the present work, this condition has been relaxed, in a manner similar to that of Smith & Stansby (1988). At each time step, the elemental vortices are created having the circulation of each vortex segment on the surface of a baffle; vortices on the upstream faces of the baffles are released into the flow to simulate the formation of the boundary layers. Interactions between the elemental vortices in the recirculating flow in the cavity region between the baffles can have an unphysically disruptive influence on the sensitive separating shear layer unless very large numbers of vortices are employed. As this was not computationally feasible in the present study, the time-mean vorticity in the cavity region predicted from an initial simulation was fixed on a 21×21 grid. This representation provided the approximately correct velocity contribution to the shear layer under consideration from the cavity region without introducing instabilities due to numerical noise; satisfactory vortex development was then predicted in the shear layer separating from the upstream baffle.

The elemental vortices are potential vortices with smoothed cores (Rankine profile) of radius $0{\cdot}03b$, where b is the spacing between the upstream and downstream baffles. Test cases with larger and smaller smoothing cores showed that the formation of the large-scale vortex structures was insensitive to the exact smoothing value used. The vortices are advected using a second-order Adams-Bashford scheme; a time-step of $0{\cdot}01(b/v_\infty)$ is used, where v_∞ is the upstream flow velocity. As mentioned above, prediction of the level of the resonant acoustic particle velocity amplitudes was not attempted; these amplitudes were determined from the empirical data. For input to the numerical model, the value for the amplitude of the acoustic particle velocity at the centre of the duct midway between the baffles is set to $0{\cdot}1v_\infty$, which is in the middle of the empirical range. Amplitudes fifty per cent higher and lower than this value were also used in the model to test the sensitivity of the results; near identical results were obtained. To economize on the number of computations required, the vortices are merged according to an exponential weighting function of the distance downstream of the upstream baffle.

4.3. Interaction of Flow and Sound

Howe (1975, 1980) showed that when an acoustic oscillation occurs in an inviscid, isentropic but rotational flow, then an instantaneous acoustic power P is generated in a volume V, which is given by

$$P = -\rho_0 \int \boldsymbol{\omega} \cdot (\mathbf{v} \times \mathbf{u}) \, \mathrm{d}V \tag{6}$$

where $\mathbf{v}$ is the fluid velocity, $\boldsymbol{\omega} = \nabla \times \mathbf{v}$ is the vorticity, $\mathbf{u}$ is the acoustic particle velocity and ρ_0 is the mean density of the fluid.

When the vorticity is "compact", that is when the vorticity extends over a region which is small relative to the acoustic wavelength, then the acoustic power per unit length of vortex tube generated by a vortex reduces to

$$P = \rho_0 \Gamma \mathbf{k} \cdot (\mathbf{v} \times \mathbf{u}), \tag{7}$$

where Γ is the circulation of the vortex and $\mathbf{k}$ is the unit vector normal to the plane of the flow.

For the present analysis, where the flow near the downstream baffle will be identified as an acoustic source, it is useful to rewrite the above expression for acoustic power P in terms of the phase of arrival of the vortex at that baffle relative to the sound cycle. P is oscillatory over time because of the oscillation of the acoustic particle velocity; to separate this oscillatory term, first $\mathbf{u}$ is factorized:

$$\mathbf{u} = \mathbf{u}_0 \sin[2\pi f(\tau - \tau_0) + h], \tag{8}$$

where $\mathbf{u}_0$ is the steady amplitude of the sound field, f is its frequency and τ_0 is the time at which the vortex is directly above the downstream baffle. Here, h is the phase of the acoustic cycle at which the vortex passes over the downstream baffle. Then

$$P = Q \sin[2\pi f(\tau - \tau_0) + h], \tag{9}$$

where

$$Q = -\rho_o \Gamma |\mathbf{v}| \, |\mathbf{u}_0| \sin \epsilon \tag{10}$$

and ϵ is the angle between $\mathbf{v}$ and $\mathbf{u}_0$.

Two simple examples will serve to explain the physics of equations (9) and (10). First, if a vortex travels *parallel* to the local acoustic particle velocity amplitude $\mathbf{u}_0$, then the angle ϵ between the vortex velocity $\mathbf{v}$ and $\mathbf{u}_0$ is zero. Therefore, Q in (10) is zero and according to (9), no instantaneous acoustic power P is generated. Consequently, the net acoustic energy generated over an acoustic cycle is zero. This situation arises, for example, if the vortex is travelling along a duct in a longitudinal standing wave far away from duct modifications. Second, if a vortex travels *orthogonal* to the local acoustic particle velocity (i.e. $\epsilon = \pm \pi/2$), the amplitude of Q is maximum and the instantaneous acoustic energy P oscillates with time. If the vortex velocity and the local acoustic particle velocity amplitude remain constant, then the integrated energy over an acoustic cycle is zero. Therefore, for net acoustic energy to be generated over a cycle, Q must vary, which occurs most readily near a duct modification (e.g. a baffle) where the angle between the local acoustic particle velocity and the vortex velocity can vary rapidly in space. In the present investigation, a net acoustic energy generated over a cycle will be shown to be possible when a vortex passes the downstream baffle.

The sign and amount of acoustic energy generated by vortex structures will be shown to be critically dependent on the phase h of the acoustic cycle at the instant of arrival of a vortex structure at the downstream baffle. That is, the phase offset h plays a crucial role in the aeroacoustic process. Some key values of h are: $h = 0$, the resonant acoustic particle velocities are zero everywhere and changing to a direction which augment the mean flow; $h = \pi/2$, the acoustic particle velocities are maximum and in the flow direction; $h = \pi$, the acoustic particle velocities are zero everywhere and beginning to oppose the mean flow; $h = 3/2\pi$, the acoustic particle velocities are maximum in the upstream direction.

The excitation of an acoustic resonance from an initially low level is a complex transient process. Linear analysis of an initial excitation of a resonant acoustic mode has been performed by Chung & Sohn (1986) and Flandro (1986). In the present work, attention is focussed on whether a resonance can be sustained at the established

observed levels and the nature of the dominant sources of sound in the flow that can sustain the resonance. A resonant sound field will be assumed to be present, and in some cases the predicted mean acoustic energy per cycle generated by the flow will be found to be relatively low or negative. Although the vortical structures that evolve as a result of the assumed resonance in these cases are fictitious, the result shows that such a resonance cannot exist and describes potential acoustic sinks. To determine whether the predicted acoustic energy per cycle generated by the flow is consistent with observed resonances at various flow velocities, the following strategy is adopted.

(i) The principally longitudinal acoustic resonant mode is predicted using the finite element technique.

(ii) The predicted resonant acoustic field at the observed sound pressure level is incorporated in the flow model, resulting in the synchronized shedding of large-scale vortices from the leading baffle.

(iii) The acoustic energy per cycle generated by the entire flow is then calculated.

(iv) If the acoustic energy per cycle generated by the flow is relatively low, then resonance is deemed not to be sustainable.

(v) This procedure is repeated for a number of different flow velocities. The flow velocities at which peaks in the generated acoustic energy per cycle are maxima are compared with those velocities at which resonances are observed.

(vi) The instantaneous acoustic power generated by a single large-scale vortex during its passage past the downstream baffle is predicted; this provides insight into the source of the acoustic resonance and why the resonance is observed for only certain discrete velocity ranges.

5. RESULTS

5.1. Predicted Resonant Acoustic Field

The local acoustic particle velocity magnitudes, predicted by the finite element method (Section 4.1) for the resonant longitudinal field (having a wavelength approximately equal to the length of the duct) with baffles installed (Section 4.1), are shown in Figure 4(a). The velocity directions are generally horizontal except near the baffles where significant vertical components are found. The acoustic particle "streamlines" calculated using the potential flow solution (Section 4.2.1) approximation are shown in Figure 4(b).

5.2. Experimentally Observed Resonances

The relationship between resonance and flow velocity is most clearly shown in terms of an acoustic Strouhal number St_a. This is formed by multiplying the sound frequency f by the distance between the baffles b (130 mm) and dividing this product by the average velocity upstream of the baffles. The reference length is chosen to be the distance between the baffles rather than the acoustic wavelength because it will be shown that the time taken by a vortex to traverse this spacing determines whether the acoustic resonance can be sustained.

The power spectra of the signal detected by the microphone located between the baffles when resonance occurs are shown in Figure 5. Frequency, which is normally plotted on the horizontal axis, is replaced by the acoustic Strouhal number St_a. Peaks in the spectra at acoustic Strouhal numbers of 11·0, 7·7 and 4·7 indicate the amplitude of the resonances which are at the same frequency ($\simeq 100$ Hz) and are the resonant

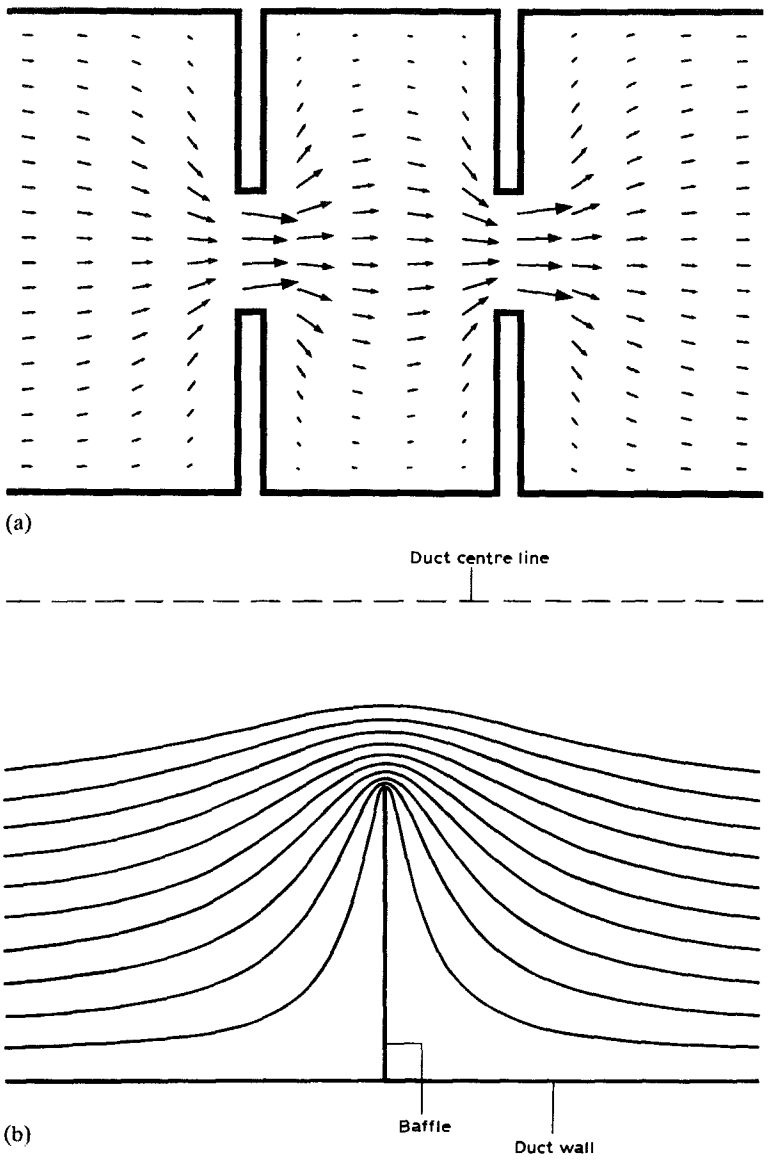

Figure 4. (a)Acoustic particle velocity vectors predicted by the finite element method at a phase of the sound cycle where the acoustic particle velocity is greatest in the downstream direction; (b) predicted acoustic particle "streamlines" near an isolated baffle used for the single vortex model.

mode described in Section 5.1. They occur at different mean upstream flow velocities of 1·2, 1·7 and 2·7 m/s, respectively. At the highest flow velocity, harmonics of the primary peak also appear but at considerably lower amplitude than the primary peak.

Three different multiple flash photographs of the flows between the baffles are shown in Figure 6 for the conditions corresponding to the sound pressure level peaks in the spectra shown in Figure 5. In each photograph the resonant acoustic mode and the frequency is the same ($\simeq$ 100 Hz). It is clear that at acoustic Strouhal numbers of 11·0, 7·7 and 4·7, there are, respectively three, two or one pair(s) of vortices between the baffles, as found also by Nomoto & Culick (1982).

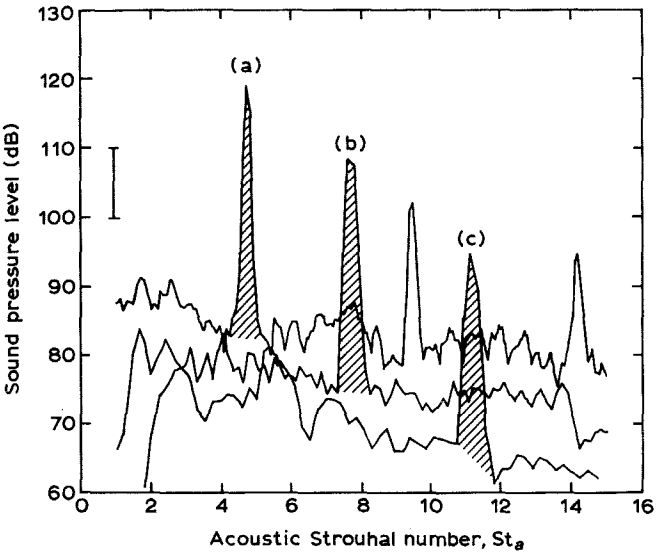

Figure 5. Plot of the power spectrum of the signal from the microphone located between the baffles at the acoustic Strouhal numbers (a) $St_a = 4{\cdot}7$; (b) $St_a = 7{\cdot}7$; (c) $St_a = 11{\cdot}0$. Each plot has a marked peak (shaded) at the resonant frequency; the other major peaks shown in the spectrum are harmonics.

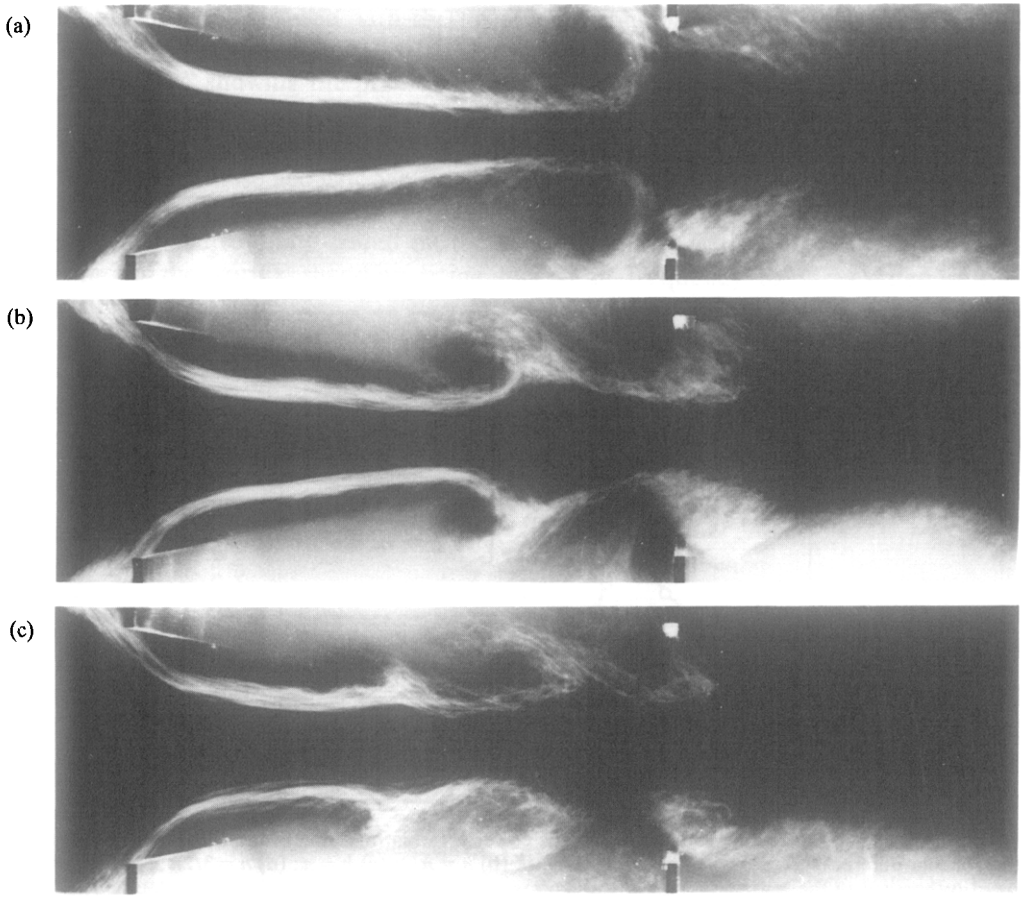

Figure 6. Photographs using smoke visualisation of the flow for the first three peaks in sound pressure level found at the acoustic Strouhal numbers (a) $St_a = 4{\cdot}7$; (b) $St_a = 7{\cdot}7$; (c) $St_a = 11{\cdot}0$.

5.3. Single Point Vortex Model

Figure 7 shows the instantaneous acoustic power generated by a vortex, having infinitesimal strength and following a horizontal path, as it passes over the downstream baffle; the baffle and vortex are both surrounded by a longitudinal acoustic field. The instantaneous power is shown for four different values of the phase offset h, which specifies the phase of the acoustic field at the instant the vortex passes over the downstream baffle [see equation (8)]. It is only when the vortex is near, but not directly above, the baffle that the angle ϵ [see equation (10)] is significant and the absolute value of P is relatively large. That is, the direction of motion of the vortex and the local

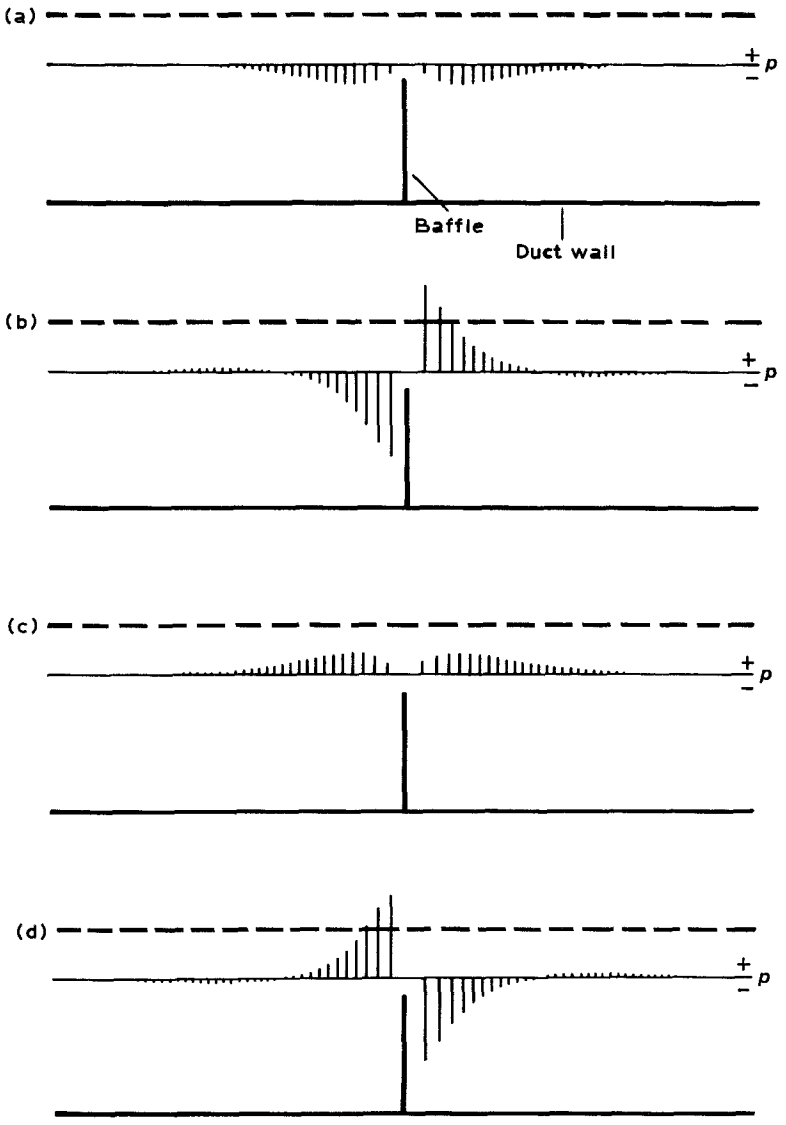

Figure 7. Plots of predicted instantaneous acoustic power P (arbiatrary units) for a single vortex passing a baffle for four different values of the phase h: (a) $h = 0$; (b) $h = \pi/2$; (c) $h = \pi$; (d) $h = 3/2\pi$; | line segments plotted orthogonal to the horizontal path of the vortex have lengths proportional to the value of P at that point of the trajectory.

acoustic particle velocity direction are non-parallel on either side of the baffle and acoustic power generation is possible. Far upstream and downstream, and directly above the baffle, the two directions are parallel and no acoustic power generation possible. The sign of the instantaneous acoustic power generated depends on the sense of the local acoustic particle velocity, which in turn depends on the phase offset h. As the phase offset h is varied, different combinations of positive and negative peaks in the time history of the acoustic power generation appear. Two equal positive peaks are found for $h = \pi$ and two equal negative peaks are found for $h = 0$.

The net acoustic energy generated by a point vortex during its passage past the baffle is a sinusoidal function of the phase offset h, under the present assumptions. This can be easily shown by integrating equation (9) over time. The net acoustic energy reaches its maximum value (positive) when $h = \pi$ and its minimum value (negative) when $h = 0$. For $h = \pi/2$ and $h = 3/2\pi$, the net generated acoustic energy over time is zero.

5.4. Vortex Cloud Model

From the vortex cloud model, the predicted acoustic energy output per acoustic cycle due to the entire flow is shown in Figure 8 over a range of acoustic Strouhal numbers. The total power was obtained by summation of the individual powers (7) over all the vortices in the flow over ten consecutive acoustic cycles. The acoustic Strouhal numbers at which peaks in the acoustic energy per cycle generated by the vortex clouds occur are found to coincide well with the observed values of 7·7 and 4·7; a predicted third peak near the observed value of 11·0 is only slightly resolved.

"Snapshots" showing the predicted elemental vortex positions are shown in Figure 9 for the acoustic Strouhal numbers corresponding to peaks in the time-mean sound pressure level, and the same phase of the acoustic cycle, as for the photographs shown in Figure 6. At these acoustic Strouhal numbers of 4·7, 7·7 and 11·0, there are one, two and three pair(s) of vortices, respectively, between the baffles. There is clearly a feedback of the resonant sound on the flow separating at the upstream set of baffles, leading to the vortex shedding being locked in frequency to the excited resonant acoustic mode.

Figure 10 shows the predicted instantaneous acoustic power output P generated by the flow over a number of cycles for two acoustic Strouhal numbers, $St_a = 4{\cdot}7$ and $St_a = 6{\cdot}0$, corresponding to a maximum and minimum, respectively, of the predicted

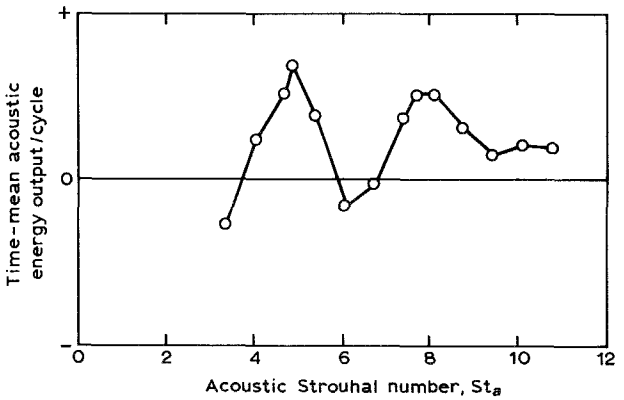

Figure 8. Predicted generated acoustic energy per cycle (arbitrary units) due to the entire flow derived from the vortex cloud model over a range of acoustic Strouhal numbers.

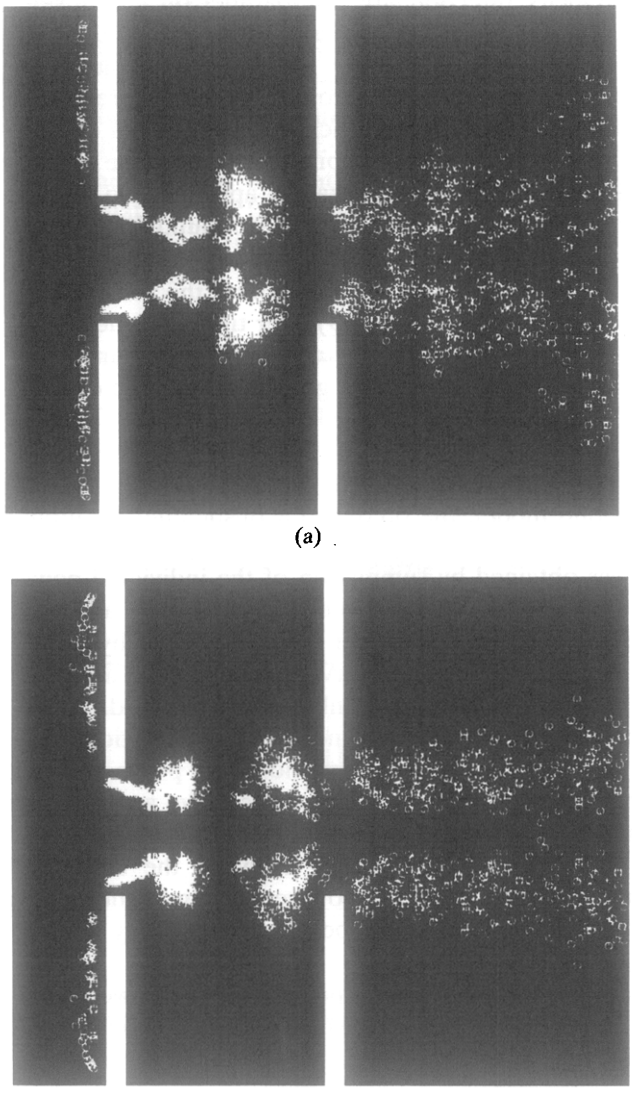

Figure 9. Predicted vortex positions (superimposed from the same phase of the acoustic cycle over five consecutive acoustic cycles) corresponding to Figure 6 for the three acoustic Strouhal numbers associated with peak acoustic resonances: (a) $St_a = 4{\cdot}0$; (b) $St_a = 7{\cdot}7$; (c) $St_a = 11{\cdot}0$. Elemental vortex positions are at centres of circles.

acoustic energy per cycle generated. The average generated acoustic energy per cycle is found to be negative when $St_a = 6{\cdot}0$ (resonance not observed) and positive when $St_a = 4{\cdot}7$ (resonance observed).

Figure 11(a, b) shows sequences of "snapshots", or instantaneous plots, highlighting the position of a large-scale vortex structure as it passes across the top of the downstream baffle, for $St_a = 4{\cdot}7$ and $6{\cdot}0$. It is useful in interpreting these figures to note that for a vortex travelling left to right, positive instantaneous acoustic power P is generated if there is a component of the local acoustic particle velocity $\mathbf{u}$ upwards and negative P if there is a component of $\mathbf{u}$ downwards. For each Strouhal number, the first

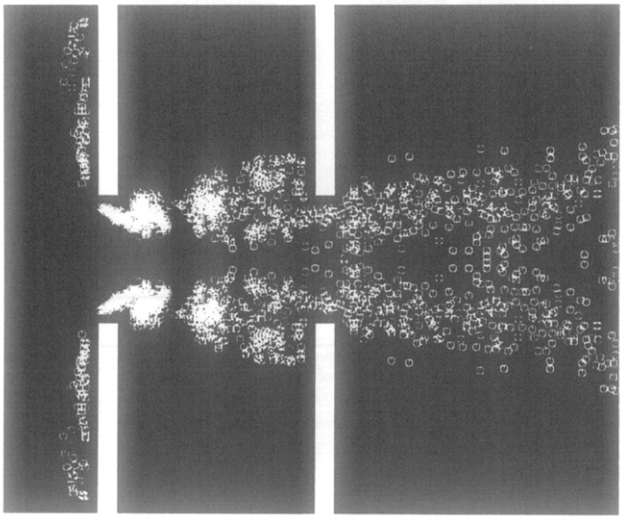

(c)

Figure 9. (*continued*)

"snapshot" is such that the acoustic particle velocity is zero and about to become positive in the downstream direction. The following "snapshots" are separated in phase angle by $\pi/2$. The phase h (see equation (8)) of the acoustic cycle at which the vortex arrives at the top of the second baffle has been stressed in the preceding description as being an important indicator of the sign and amount of acoustic power that is expected to be generated by a vortex in its passage past the downstream baffle. A study of the complete selection of "snapshots" of the flow, a sample of which are shown in Figure 11(a, b), indicates that the phase offset h is approximately π for $St_a = 4{\cdot}7$ and approximately 0 for $St_a = 6{\cdot}0$. Figure 11 (a, b) also indicates the flow velocity and local acoustic particle velocity at the vortex cloud centroid for the cases when the acoustic particle velocity is nonzero.

The predicted history of acoustic power generation by a large-scale vortex structure shed from the upstream baffle and passing the downstream set of baffles is shown in

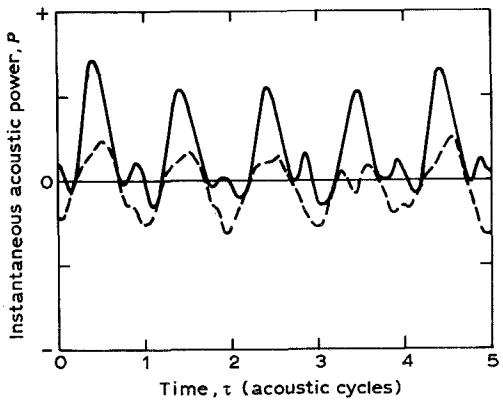

Figure 10. Predicted instantaneous acoustic power P (arbitrary units) generated by the entire flow at two different acoustic Strouhal numbers corresponding to a maximum and a minimum of the generated acoustic energy per cycle: ———, $St_a = 4{\cdot}7$ (maximum); — — —, $St_a = 6{\cdot}0$ (minimum).

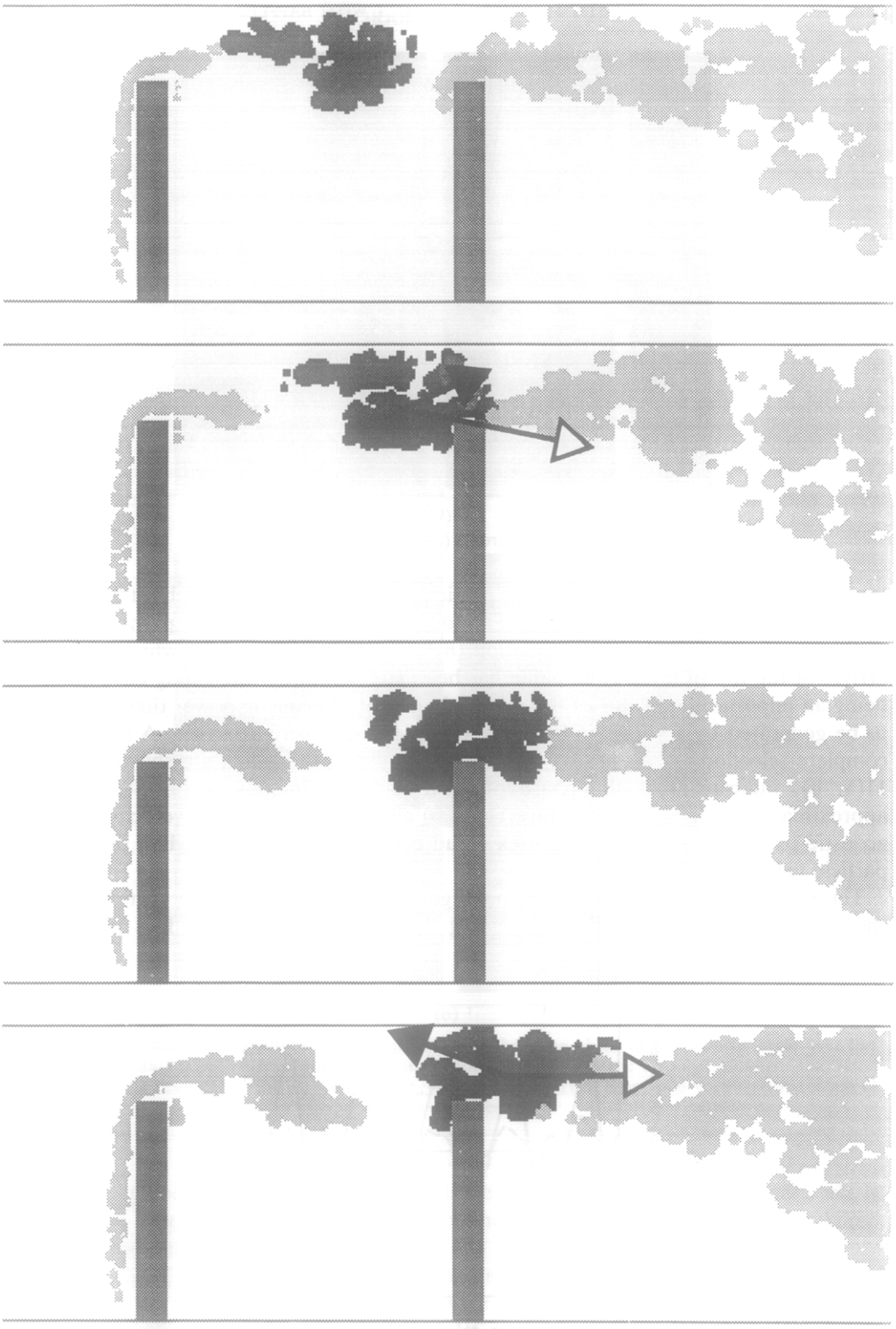

(a)

Figure 11. Predicted instantaneous flow structures (superimposed from the same phase of the acoustic cycle over five consecutive acoustic cycles) at quarter acoustic cycle intervals for the acoustic Strouhal numbers (a) $St_a = 4{\cdot}7$ and (b) $St_a = 6{\cdot}0$; —▷, direction and relative magnitude of vortex centroid velocity;

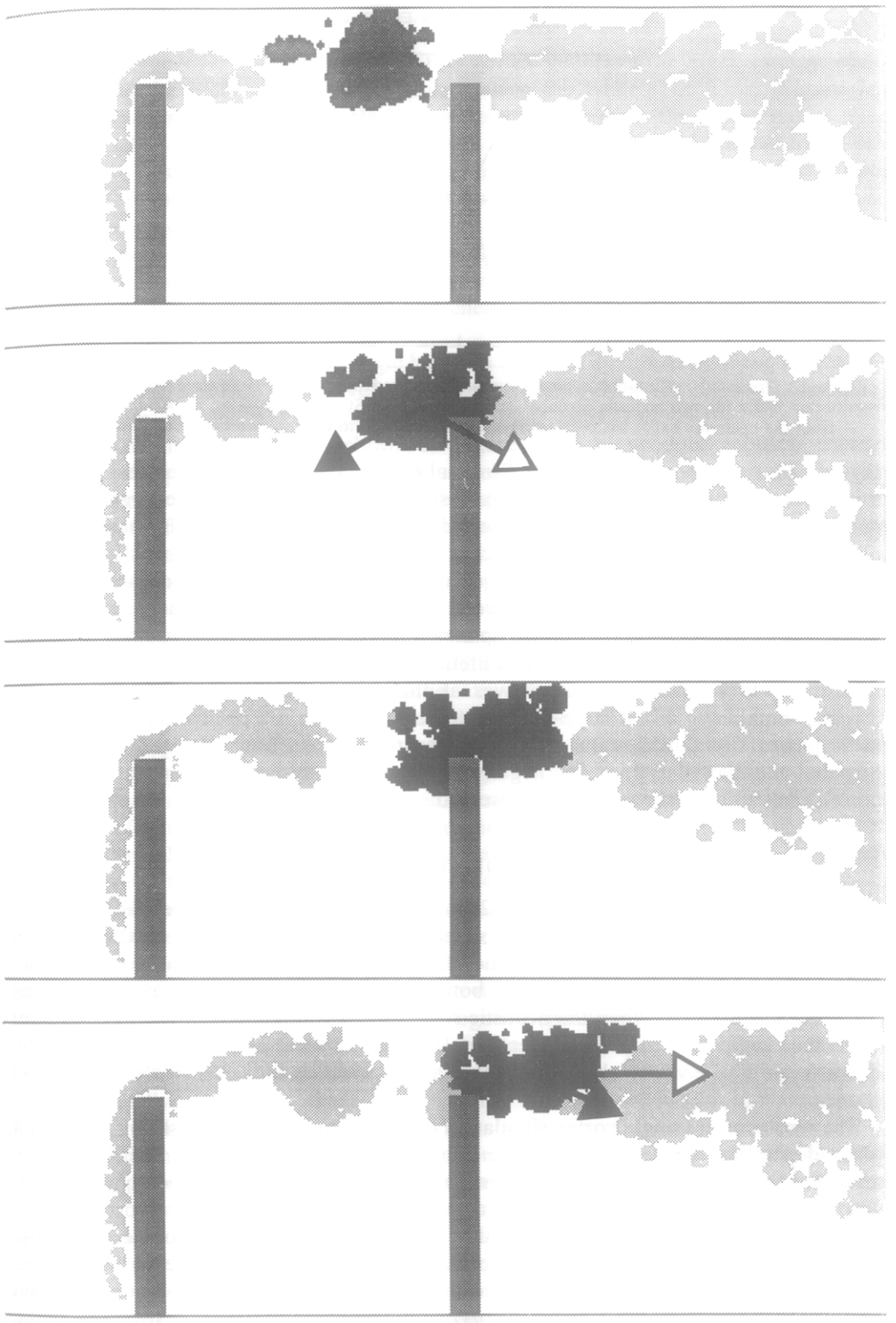

(b)

→, direction and relative magnitude of the acoustic particle velocity at the vortex centroid (scaled up by a factor of 5). The vortex cloud under consideration has been highlighted by plotting a shaded circle at the position of each of its constituent elemental vortices.

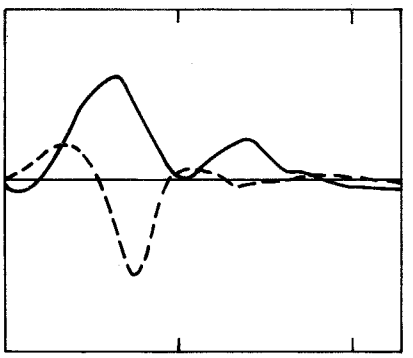

Figure 12. Predicted instantaneous power output generated by a single large-scale vortex passing the downstream baffle for two acoustic Strouhal numbers: ———, $St_a = 4{\cdot}7$; — — —, $St_a = 6{\cdot}0$. The distance from the upstream baffle has been normalized with respect to the distance between the baffles.

Figure 12 for the above two acoustic Strouhal numbers of 4·7 and 6·0, corresponding to a local maximum and a local minimum, respectively, of the acoustic energy per cycle generated by the flow. The resonant sound field at the assumed level determines the phase of the acoustic cycle during which a new vortex grows in the shear layers shed from the upstream set of baffles. This phase is independent of the acoustic Strouhal number; as a result of the angle between the vortex velocity and the local acoustic particle velocity, the region near the upstream baffle is a small acoustic sink. Whether net positive energy is generated over a lifetime of a vortex depends on the phase of the acoustic cycle when the vortex arrives at the downstream baffle. For an acoustic Strouhal number of 4·7, a large-scale vortex contributes a net positive acoustic energy as it passes the downstream set of baffles (resonance observed); for an acoustic Strouhal number of 6·0, a net negative acoustic energy contribution results which corresponds to no resonance being observed.

6. DISCUSSION

The results of Nomoto & Culick (1982) and the experiments described in this paper reinforce the notion that the existence of acoustic resonance depends on the phase of the acoustic cycle at which vortices, shed from the upstream baffle each sound cycle, arrive at the downstream baffle. In both sets of experiments, no regular vortex shedding was detected when the acoustic resonance was not excited. This is consistent with the idea that a phase-dependent acoustic source can exist at a location downstream of the vortex shedding region, as proposed by Stokes & Welsh (1986) and Stoneman *et al.* (1988).

The results of the single vortex simulation described here (Figure 7) show how such a phase-dependent source can exist. The phase of the acoustic cycle at which a vortex arrives at the downstream baffle is determined by the phase offset h [see equation (8)]. That is, the value of the instantaneous acoustic power P generated by a vortex is very dependent on the direction and amplitude of the acoustic particle velocities when the vortex passes a given point. The net acoustic energy generated by the vortex passing the baffle is equal to the integral of P over time. For the cases shown in Figure 7(b) and (d), where $h = \pi/2$ and $h = 3\pi/2$, respectively, the vortex is passing over the baffle when the local acoustic particle velocity is at a maximum and the integral is zero due to antisymmetry. That is, for the cases where the acoustic particle velocity is at a maximum when the vortex reaches the downstream baffle, the vortex generates no net

acoustic energy over its time history. The vortex generates as much energy while approaching the baffle as it absorbs while leaving the baffle. For $h = \pi$ (Figure 7c) maximum acoustic energy per cycle is generated. In this case, the vortex passes over the baffle when the acoustic particle velocity is zero everywhere and is about to change direction to upstream and oppose the mean flow. This value of the phase offset allows $\sin \epsilon$ [see equation (10)] to remain negative on both sides of the downstream baffle as the vortex cuts across the acoustic particle velocity field lines leading to positive contributions to the acoustic energy while both approaching and leaving the baffle. A maximum net acoustic energy output results. For $h = 0$, the reverse is true. Here $\sin \epsilon$ remains positive during the traversal and energy absorption takes place both before and after crossing the baffle.

In the single vortex model, the angle between the velocity direction of the vortex and that of the local acoustic particle velocity are significant only in the region of the baffle. That is, the vortex, which follows a horizontal path, cuts across the acoustic "streamlines" near the baffle (shown in Figure 4(b)) to produce acoustic energy, according to equations (9) and (10). This model explains the basic concepts behind the acoustic energy generation process well but, importantly, it cannot predict the variation of the phase offset h as a function of Strouhal number. The vortex cloud model enables this to be done.

The results of the vortex cloud model support the concept of an acoustic source which is phase-dependent. The shedding rate of the vortex clouds from the upstream baffle is predicted to be locked to the sound frequency in the presence of the strong sound field; the phase of the acoustic cycle at which these clouds begin to grow is observed and predicted to be the same for different acoustic Strouhal numbers. However, the phase of the acoustic cycle at which a cloud arrives at the downstream baffle is strongly dependent on the acoustic Strouhal number (and therefore flow velocity). Comparing the observed flows in Figure 6 with the predicted flows in Figure 9 shows that the vortex cloud model predicts satisfactorily the occurrence of different numbers of vortices between the baffles at the appropriate locations for each of the acoustic Strouhal numbers at which a peak sound pressure level is observed. Furthermore, the acoustic Strouhal numbers (4·7 and 7·7) at which predicted peaks in the acoustic energy per cycle is generated by the flow (Figure 8) correspond very closely to those at which peaks in the sound pressure level are measured (Figure 5).

For $St_a = 4{\cdot}7$, Figure 11(a) shows that the vortex cloud centre near the downstream baffle moves from upstream of the baffle to downstream of the baffle as the acoustic particle velocity changes from positive to negative (positive refers to the downstream direction). Interpreted in terms of the single vortex model, the phase offset in this case is $h = \pi$, corresponding to the case where maximum net acoustic energy is generated. Experimentally, a peak in the sound pressure level was observed at this acoustic Strouhal number (Figure 5).

A similar phenomenon occurs for the resonance occurring at an acoustic Strouhal number of 7·7 at the correspondingly lower flow velocity. In this case, the vortex cloud model also predicts that the vortex cloud passes over the downstream baffle approximately when the acoustic particle velocity is changing sign from positive to negative. This supports the predictions of the single vortex model, and confirms the predicted phase relationship between the acoustic field and the arrival of the vortex approaching the downstream baffle necessary to maximize the production of net acoustic energy and therefore sound pressure level.

The instantaneous acoustic power generated for $St_a = 4{\cdot}7$ is found to have two positive peaks each sound cycle (Figure 12), as predicted also by the single vortex

model in Figure 7(c). This results in a net positive acoustic energy being generated per acoustic cycle at this acoustic Strouhal number, as seen in Figure 8. However, in contrast with the single vortex model results, the peaks are not equal in magnitude. More detailed analysis and viewing of videotape recordings of the dynamic simulation reveal that, as a result of complex interaction between the vortex cloud and the downstream baffle and loss of vorticity into the cavity, the net circulation of the vortex cloud is decreased as it passes the downstream baffle. Consequently, the second peak is not as substantial as the first. Nonetheless, although slightly modified in detail, the single vortex model prediction of positive contributions from both sides of the baffle in the resonant situation is borne out by the more sophisticated model.

For $St_a = 6{\cdot}0$, the vortex cloud arrives at the downstream baffle half a sound cycle later [Figure 11(b)] than for the case where $St_a = 4{\cdot}7$, resulting in a net negative generation of acoustic energy (Figure 12). The acoustic resonance would not be sustained under these circumstances, which is consistent with the observation of no recorded resonance at this acoustic Strouhal number. Notice that for this Strouhal number (6·0) the second negative peak in Figure 12 (after the vortex cloud has passed the second baffle) is almost nonexistent, which differs from the result of the single point vortex model (Figure 7(a)). The difference seems to be due in part to the amount of circulation retained by the vortex as it passes the downstream baffle; the circulation is unchanged in the point vortex model, whereas it decreases in the vortex cloud model. Some of this circulation decrease results from the sound field pushing part of the vortex cloud into the cavity as it approaches the downstream baffle. Consequently, much less of the total circulation passes over the baffle at this Strouhal number relative to that for the resonant Strouhal number leading to less absorption of acoustic energy than would otherwise occur. However, the net source of acoustic energy is still negative indicating that the hypothetical loud acoustic resonance assumed in the model cannot be sustained at this acoustic Strouhal number. This means that the sound pressure level would not build up to loud resonant levels in practice, as verified by the experiments. The linear stability theory of Flandro (1986) also indicates that certain resonant modes of a rocket chamber will grow in amplitude in only certain ranges of the Strouhal number.

It is therefore proposed that the influence of the resonant sound field in synchronising the vortex shedding is a vital part of the overall resonance process. This is effectively acoustic feedback. Nomoto & Culick (1982) cast doubt on the role of feedback, saying that the distance from source to feedback site is too small for compressibility to be important. This distance, however, is not the one that matters. The feedback is via a resonance, which means that most of the sound energy which influences vortex shedding at any one time was generated in previous cycles, and has been reflected, usually many times, from the duct terminations.

Finally, it is noted that the present investigation reveals an acoustic phenomenon which is fundamentally similar to the case of flow past a square leading edge plate (Stokes & Welsh 1986). In each case, the vortex shedding point (upstream baffle or square leading edge of plate) is remote from a downstream acoustic source region (downstream baffle or trailing edge of plate). The acoustic resonance can be sustained only when the vortices, shed at the acoustic frequency via feedback of the resonant acoustic mode, arrive at the downstream source region at a particular phase of the acoustic cycle. The phase of arrival of a vortex at the downstream source region is a function of the flow velocity; the particular phase required for acoustic energy to be generated can occur for a number of different flow velocities. Therefore, acoustic resonance is observed over discrete velocity ranges in both cases even though the plate

and baffle geometries are different and the present resonant acoustic mode is principally longitudinal rather than transverse.

7. CONCLUSIONS

An essentially longitudinal resonant acoustic mode can be excited in a duct by flow over two sets of baffles. Peak sound pressure levels of this mode are observed to occur when large-scale vortices, formed in the shear layers separating from the upstream set of baffles, approach the downstream set of baffles at a particular phase of the induced resonant acoustic cycle.

Incorporation of Howe's (1975) theory of resonant sound into two different flow models enables the determination of the sound sources in the flow and an explanation of the occurrence of peak sound pressure levels at particular flow velocities.

The feedback of the sound field, via a velocity perturbation, on the separating shear layer from the upstream baffle synchronizes the vortex shedding to the sound, resulting in vortices being formed at the same instant of the acoustic cycle independently of the acoustic Strouhal number. The generation of acoustic energy necessary to sustain an acoustic resonance has been shown to depend on the phase of the acoustic cycle at which a vortex passes the downstream baffle. This phase is a function of the time taken for a vortex to reach the downstream baffle, which in turn depends on the acoustic Strouhal number. This explains why acoustic resonance can only be sustained for particular acoustic Strouhal numbers.

ACKNOWLEDGEMENT

The authors wish to thank Mr N. B. Hamilton for photographing the flows described in the paper.

REFERENCES

ARCHIBALD, F. S. 1975 Self-excitation of an acoustic resonance by vortex shedding. *Journal of Sound and Vibration* **38,** 81–103.

BROWN, R. S., DUNLAP, R., YOUNG, S. W. & WAUGH, B. G. 1981 Vortex shedding as a source of acoustic energy in segmented solid rockets. *Journal of Spacecraft and Rockets* **18,** 312–319.

BLEVINS, R. D. 1985 The effect of sound on vortex shedding from cylinders. *Journal of Fluid Mechanics* **61,** 217–237.

CHUNG, T. J. & SOHN, J. L. 1986 Interactions of coupled acoustic and vortical instability. *AIAA Journal* **24,** 1582–1596.

CUMPSTY, N. A. & WHITEHEAD, D. S. 1971 The excitation of acoustic resonances by vortex shedding. *Journal of Sound and Vibration* **18,** 353–369.

FLANDRO, G. A. 1986 Vortex driving mechanism in oscillatory flows. *Journal of Propulsion and Power* **2,** 206–214.

HARRIS, R. E., WEAVER, D. S. & DOKAINISH, M. A. 1988 Unstable shear layer oscillations past a cavity in air and water flows. In *Proceedings of* 1988 *International Symposium on Flow-Induced Vibration and Noise*; *Vol.* 6: *Acoustic Phenomena and Interaction in Shear Flows over Compliant and Vibrating Surfaces* (eds W. L. Keith, E. M. Uram & A. J. Kalinowski), pp. 13–24. New York: ASME.

HEGDE, U. C. & STRAHLE, W. C. 1985 Sound generation by turbulence in simulated rocket motor cavities. *AIAA Journal* **23,** 71–77.

HOWE, M. S. 1975. Contributions to the theory of aerodynamic sound, with application to excess jet noise and the theory of the flute. *Journal of Fluid Mechanics* **71,** 625–673.

HOWE, M. S. 1980 The dissipation of sound at an edge. *Journal of Sound and Vibration* **70,** 407–411.

JOHNSON, C. O. & LOERHRKE, R. I. 1984 An experimental investigation of wake edge tones. *AIAA Journal* **22,** 1249–1253.

LEWIS, R. I. 1981 Surface vorticity modelling of separated flows from two-dimensional bluff bodies of arbitrary shape. *Journal of Mechanical Engineering Science* **23,** 1–23.

NOMOTO, H. & CULICK, E. C. 1982 An experimental investigation of pure tone generation by vortex shedding in a duct. *Journal of Sound and Vibration* **84,** 247–252.

PARKER, R. 1966 Resonant effects in wake shedding from parallel plates: some experimental observations. *Journal of Sound and Vibration* **4,** 62–72.

PARKER, R. 1967 Resonant effects in wake shedding from parallel plates: calculation of resonant frequencies. *Journal of Sound and Vibration* **5,** 330–343.

PARKER, R. 1969 Discrete frequency noise generation due to flow over blades, supporting spokes and similar bodies. ASME, Paper No. 69–WA/GF13.

PARKER, R. & GRIFFITHS, W. M. 1968 Low frequency resonant effects in wake shedding from parallel plates. *Journal of Sound and Vibration* **7,** 371–379.

SMITH, P. A. & STANSBY, P. K. 1988 Impulsively started flow around a circular cylinder by the vortex method. *Journal of Fluid Mechanics* **194,** 45–77.

STOKES, A. N. & WELSH, M. C. 1986 Flow-resonant sound interaction in a duct containing a plate, II: square leading edge. *Journal of Sound and Vibration* **104,** 55–73.

STONEMAN, S. A. T., HOURIGAN, K., STOKES, A. N. & WELSH, M. C. 1988 Resonant sound caused by flow past two plates in tandem in a duct. *Journal of Fluid Mechanics* **192,** 455–484.

WELSH, M. C. & GIBSON, D. C. 1979 Interaction of induced sound with flow past a square leading edged plate in a duct. *Journal of Sound and Vibration* **67,** 501–511.

WELSH, M. C., STOKES, A. N. & PARKER, R. 1984 Flow-resonant sound interaction in a duct containing a plate, Part I: semi-circular leading edge. *Journal of Sound and Vibration* **95,** 305–323.

WELSH, M. C., HOURIGAN, K., WELCH, L. W., DOWNIE, R. J., THOMPSON, M. C. & STOKES, A. N. 1990. Acoustic and experimental methods: the influence of sound on flow and heat transfer. *Experimental Thermal and Fluid Science* **3,** 138–152.

WARSI, Z. U. A. 1982 Basic differential models for coordinate generation. In *Numerical Grid Generation*, (ed. J. F. Thompson), pp. 41–77. Amsterdam: North-Holland.

ZIENKIEWICZ, O. C. 1978 *The Finite Element Method*. New York: McGraw-Hill.